MOLECULAR AND CELLULAR BIOLOGY, Jan. 2007, p. 170–181 Vol. 27, No. 1
0270-7306/07/$08.00+0 doi:10.1128/MCB.01456-06

The Mitogen-Activated Protein Kinase (MAPK)-Activated Protein Kinases MK2 and MK3 Cooperate in Stimulation of Tumor Necrosis Factor Biosynthesis and Stabilization of p38 MAPK▽

N. Ronkina,[1] A. Kotlyarov,[1] O. Dittrich-Breiholz,[2] M. Kracht,[2] E. Hitti,[1] K. Milarski,[3] R. Askew,[3] S. Marusic,[4] L.-L. Lin,[4] M. Gaestel,[1]* and J.-B. Telliez[4]

Institute of Biochemistry[1] and Institute of Pharmacology,[2] Medical School Hannover, Carl-Neuberg-Strasse 1, 30625 Hannover, Germany, and Biological Technology[3] and Inflammation Department,[4] Wyeth Research, 200 Cambridge Park Drive, Cambridge, Massachusetts 02140

Received 7 August 2006/Returned for modification 15 September 2006/Accepted 2 October 2006

MK2 and MK3 represent protein kinases downstream of p38 mitogen-activated protein kinase (MAPK). Deletion of the MK2 gene in mice resulted in an impaired inflammatory response although MK3, which displays extensive structural similarities and identical functional properties in vitro, is still present. Here, we analyze tumor necrosis factor (TNF) production and expression of p38 MAPK and tristetraprolin (TTP) in MK3-deficient mice and demonstrate that there are no significant differences with wild-type animals. We show that in vivo MK2 and MK3 are expressed and activated in parallel. However, the level of activity of MK2 is always significantly higher than that of MK3. Accordingly, we hypothesized that MK3 could have significant effects only in an MK2-free background and generated MK2/MK3 double-knockout mice. Unexpectedly, these mice are viable and show no obvious defects due to loss of compensation between MK2 and MK3. However, there is a further reduction of TNF production and expression of p38 and TTP in double-knockout mice compared to MK2-deficient mice. This finding, together with the observation that ectopically expressed MK3 can rescue MK2 deficiency similarly to MK2, indicates that both kinases share the same physiological function in vivo but are expressed to different levels.

Downstream of mitogen-activated protein kinases (MAPKs) different groups of MAPK-activated protein kinases (MAP KAPKs) have been defined (reviewed in reference 28). These enzymes transduce signals to target proteins that are not direct substrates of the MAPKs and, therefore, serve to relay phosphorylation-dependent signaling within MAPK cascades to diverse cellular functions. One of these groups is formed by the three MAPKAPKs, MK2, MK3 (also known as 3pK), and MK5 (also designated PRAK) (reviewed in reference 12). While MK5 is mainly activated by the atypical MAPK ERK3 (29, 30), the remaining two kinases, MK2 and MK3, are directly downstream of the MAPK p38α/β (7, 10, 24, 27, 31). Phosphorylation of MK2 and MK3 by p38α/β at two or three major regulatory sites leads to activation and coupled nuclear export of both enzymes, which are localized in the nucleus of resting cells (4, 8, 26, 36, 41).

A wide variety of substrates has been described for MK2 including proteins interacting with the cytoskeleton, such as small heat shock protein Hsp25 (33); mRNA-binding proteins, such as tristetraprolin (TTP) (6, 32); transcription factors, such as heat shock factor 1 (38); and regulators of the cell cycle and apoptosis, such as Cdc25B/C (23). The phosphorylation site recognition motifs of MK2 and MK3 are similar (20) or even identical (7). Despite the similar recognition motif, not all MK2 substrates have been described as MK3 substrates so far, probably because in most cells MK2 activity dominates and makes analysis of the minor MK3 activity dependent on antibodies which discriminate between both enzymes (7).

MK2-deficient mice are more resistant than wild type to endotoxic shock due to impaired production of cytokines such as tumor necrosis factor (TNF) (16). By genetic evidence it has been demonstrated that the mechanism by which MK2 stimulates lipopolysaccharide (LPS)-dependent TNF biosynthesis exists at the posttranscriptional level and is dependent on the adenine/uridine-rich element (ARE) in the 3′ untranslated region of TNF mRNA (25) and on the existence of the TNF mRNA-destabilizing protein TTP (15). Probably, phosphorylation of TTP by MK2 inactivates its mRNA-destabilizing activity and, in parallel, leads to stabilization and storage of phospho-TTP in complex with 14-3-3 proteins until dephosphorylation reactivates TTP and downregulates the inflammatory response (5, 6, 15, 32). Hence, phosphorylation of TTP by MK2 stabilizes TNF mRNA and stimulates its translation to TNF protein. The strong effect of deletion of MK2 on cytokine biosynthesis raised questions about the role of MK3 in this process and produced serious doubts about the functional congruence of both enzymes. Alternatively, MK3 could be responsible for residual cytokine biosynthesis or compensate an as yet undefined function of MK2 in an unrelated process such as contributing to polycomb-regulated development (37).

Here, we analyzed the role of MK3 by gene targeting strategy. By using an MK2-free genetic background, we were able to assess MK3-specific effects in vivo and, hence, to define the physiological role of this enzyme.

* Corresponding author. Mailing address: MHH, Institute of Biochemistry, Carl-Neuberg-Str. 1, D-30625 Hannover, Germany. Phone: 49 511 532 2825. Fax: 49 511 532 2827. E-mail: gaestel.matthias@mh-hannover.de.

▽ Published ahead of print on 9 October 2006.

MATERIALS AND METHODS

Generation of MK3 knockout and conditional knockout mice. MK3 knockout mice were developed by gene-targeted mutagenesis in 129SvEvBrd embryonic stem (ES) cells and with Cre-mediated recombination. A conditional knockout (CKO) allele of MK3 was designed by Wyeth, and mice carrying this CKO allele were created by Lexicon Genetics, Inc. Gene-targeted ES cell clones were identified by Southern blotting and restriction fragment length polymorphism analysis of HindIII-digested ES cell DNA using a 3′ probe external to the targeting construct in which the wild-type band is 8.6 kb and the targeted band is 10.6 kb. The CKO allele contains LoxP sites flanking exon 1 and exon 2 including the translational start site. The MK3 KO allele was converted from the CKO allele via germ line Cre-mediated deletion by crossing protamine-Cre transgenic mice (129SvEvBrd) with MK3-CKO mice. MK2 knockout mice were generated as described previously (16). $MK2^{-/-}$ mice on the C57BL/6 genetic background were bred to $MK3^{-/-}$ mice on the mixed (129Sv × C57BL/6) genetic background to obtain $MK2^{+/-}$ $MK3^{+/-}$ mice. F_2 littermates were genotyped by PCR and used in experiments. All mice used in this study were maintained under specific-pathogen-free conditions and treated in accordance with local ethical guidelines.

Genotyping of MK3 conditional allele and MK3/MK2 knockout mice. Mice were genotyped by PCR analysis of proteinase K lysate of tail biopsies. Wild-type (WT) and MK3-CKO alleles were distinguished using PCR of an amplicon spanning the 5′ LoxP insertion site with a forward primer of the sequence 5′-ATTGATTGAGCCGGGCGTGGTG-3′ and a reverse primer of the sequence 5′-CCTGTAATTGCAGCGCGAGGAA-3′, yielding 416-bp WT product and a 514-bp CKO product. The MK3 knockout (deletion) allele was distinguished from the WT allele by PCR of an amplicon spanning the deletion junction using the forward primer 5′-ATTGATTGAGCCGGGCGTGGTG–3′ and a reverse primer of the sequence 5′-CACAAGGTAGAGATTACGGCCA C-3′, yielding a 581-bp, MK3-KO-specific product. MK2 was genotyped as described previously (16).

Cell culture. Resident peritoneal macrophages were collected after intraperitoneal injection of 5 ml of Dulbecco's modified Eagle's medium (DMEM) with 10% fetal bovine serum, washed once with phosphate-buffered saline (PBS), resuspended in complete medium, and plated at 5×10^3 cells on chamber slides (Nunc, Naperville, Ill.). After 2 h at 37°C in a 95% air–5% CO_2 incubator, the macrophages were washed twice with DMEM to remove nonadherent cells and cultivated for a further 16 h prior to stimulation.

To generate bone marrow-derived macrophages (BMDMs), bone marrow cells were flushed from the femurs of mice. Cells were cultured on 10-cm dishes in DMEM supplemented with 10% heat-inactivated fetal bovine serum, 2 mM L-glutamine, 100 U/ml penicillin G, 100 μg/ml streptomycin, and 50 ng/ml recombinant macrophage colony-stimulating factor (CSF) (Wyeth, Boston, MA) for 7 days.

Primary mouse embryonic fibroblasts (MEFs) were isolated from day 13.5 mouse embryos. The heads and internal organs were removed from the embryos. The remaining tissues were then cut into small pieces, and single cells were obtained by incubation in trypsin. Cells were then cultured in DMEM containing 10% serum, 2 mM L-glutamine, 100 U of penicillin G/ml, and 100 μg of streptomycin/ml and used at passages 3 to 5. To immortalize primary MEFs, cells were cotransfected with pSV40Tag encoding simian virus 40 large T antigen and pREP8 plasmid (Invitrogen) in a 10:1 mixture; colonies were selected with 3 mM histidinol (Sigma).

Cloning and site-directed mutagenesis. The full-length murine MK3 open reading frame was amplified from cDNA clone MGC:25617 distributed by BioCat (Heidelberg/Germany) using the forward primer MK3_EcoRI (5′-CAT GGG AAT TCA TGG ATG GCG AGA CAG CAG GG-3′) and reverse primer MK3_SalI (5′-CAT GGG TCG ACG TTA CTG GTTGTT GCA TCC TTG-3′). The PCR product was digested by EcoRI/SalI and cloned into of pGEX-5x-1 (Amersham).

For cloning into pENTR/D-TOPO (Invitrogen), mouse p38 full-length cDNA was amplified by PCR using the primer pair 5′-CAC CTC GCA GGA GAG GCC CAC GTT CTA C-3′ (forward) and 5′-GGA CTC CAT TTC TTC TTG GTC AAG-3′ (reverse). The recombination reaction between the entry clone and the pDEST15 vector for glutathione *S*-transferase (GST)-tagged alpha-p38 bacterial expression was achieved with an LR Clonase Kit (Invitrogen). Site-directed mutagenesis was performed in pDEST15-alpha-p38 using a QuickChange XL site-directed mutagenesis kit (Stratagene).

GST-p38 pull-down and kinase assay. Cells cultivated overnight in serum-free medium were stimulated with either anisomycin, arsenite, or LPS (Sigma) using the concentrations and times indicated in the figures and figure legends. For kinase assays and immunoblotting, cells were lysed in 50 mM Tris-HCl (pH 7.5), 1 mM EGTA, 1 mM EDTA, 1 mM sodium orthovanadate, 50 mM sodium fluoride, 1 mM sodium pyrophosphate, 0.27 M sucrose, 1% (vol/vol) Triton X-100, 0.1% (vol/vol) 2-mercaptoethanol, and complete proteinase inhibitor cocktail (Roche, East Sussex, United Kingdom). The lysates were centrifuged at 13,000 rpm for 5 min at 4°C, and the supernatants were removed and stored at −80°C until use.

For GST pull-down 1 mg of lysate protein was incubated with 0.1 nmol of recombinant catalytically dead mutant GST-p38 (TGY/AFG) bound to glutathione-Sepharose 4B (Amersham Pharmacia Biotech). After five washes with immunoprecipitation buffer (1× Tris-buffered saline, 50 mM NaF, 1% Triton X-100, 1 mM Na_3VO_4), the beads were used for kinase assay (16) or applied for an in-gel kinase assay (9). In both cases recombinant Hsp25 was used as a substrate. Radioactivity incorporated into Hsp25 was visualized by phosphorimaging using a Fuji Bas-1500, and the signal was quantified by the use of TINA 2.09 software.

Western blotting. Soluble protein extract was run on sodium dodecyl sulfate–10% polyacrylamide gel electrophoresis (SDS–10% PAGE) gels and transferred to Hybond ECL membranes (Amersham Pharmacia Biotech). Blots were incubated for 2 h in PBS–1% Tween 20 containing 5% powdered skim milk. After three washes with PBS–1% Tween 20, membranes were incubated for 16 h with the primary antibody at 4°C and for 1 h with horseradish peroxidase-conjugated secondary antibodies (diluted 2,000-fold) at room temperature. Blots were developed with an ECL detection kit (Santa Cruz Biotechnology), and the digital chemiluminescence images were taken by a Luminescent Image Analyzer LAS-3000 (Fujifilm).

Antibodies. Anti-MK3 antibodies were raised against bacterially expressed MK3 protein. The full-length murine MK3 open reading frame was cloned in pGEX-5x-1 vector. Recombinant protein was affinity purified on glutathione-Sepharose and, the GST part was removed by Xa factor cleavage, injected into rabbits at Eurogentec (Seraing, Belgium). Antibodies that recognize p38 MAPK, phospho-p38 MAPK, MAPKAPK-2, and phospho-MAPKAPK-2 (Thr222) were from New England Biolabs. Antibody against Hsp25 was from Stressgene, and anti-phospho-Hsp25 (S86) was from Biosource. Anti-GAPDH (glyceraldehyde-3-phosphate dehydrogenase) antibody was from Chemicon. Antibodies against green fluorescent protein (GFP), actin, and horseradish peroxidase-conjugated secondary antibodies were from Santa Cruz. Anti-TTP antibody was previously described (22).

Retroviral gene transfer. Full-length murine MK2, MK3, and MK2 catalytically dead mutant (K76R) were subcloned into the pMMP-IRES-GFP (kind gift of C. Klein, MHH, Hanover) bicistronic retroviral vector upstream of the internal ribosome entry site (IRES). To obtain MEF cell lines stably expressing the kinases, retroviral supernatants were generated by transient transfection of the BD EcoPack 2-293 packaging cell line with bicistronic vectors encoding the gene of interest and GFP as marker and were used for infection. Cell lines with more than 90% GFP-positive cells were used for experiments.

Measurement of cytokines. BMDMs were scraped from 10-cm dishes, and 10^4 cells per well were transferred to a 98-well plate and incubated in 100 μl of medium for 2 h before the addition of 1 μg/ml LPS for 2 and 6 h. Murine TNF, interleukin-6 (IL-6), and CXCL1 were measured using specific enzyme-linked immunosorbent assay (ELISA) kits (R&D) according to the manufacturer's instructions. In selected experiments cytokine profiling was performed using Meso Scale Discovery (MSD) Multi-Spot plates and an MSD Sector Imager 6000 reader (Gaithersburg, MD). A total of 10 cytokines were measured simultaneously in each well of 96-well plates using an MSD 10-Plex Mouse Cytokine Panel (IL-12p40, IL-6, KC [IL-8], IL-10, IL-1, RANTES, granulocyte macrophage-CSF [GM-CSF], gamma interferon, monocyte chemoattractant protein 1, and TNF) according to the manufacturer's instructions.

Oligonucleotide DNA microarray experiments. The inflammation array (Inflmus; MWG Biotech, now sold by Ocimum as Inflammation OciChip) used in this study contains 155 validated oligonucleotide probes for 136 murine inflammatory and 19 housekeeping genes. Total RNA from MK-2-deficient and reconstituted cell lines treated as indicated in the legend of Fig. 6 was purified with a QIAGEN RNeasy kit followed by on-column DNase I digestion (QIAGEN). RNA was used to prepare Cy3-labeled cRNA by oligo(dT)-T7-primed double-stranded cDNA synthesis (cDNA synthesis system; Roche), followed by in vitro transcription with T7 polymerase (MEGAscript T7 kit; Ambion) as directed by the manufacturers. cRNA yield was determined photometrically. Equal amounts of cRNAs derived from approximately 1.5 μg of total RNA were hybridized individually to microarrays in preprepared hybridization solution (MWG Biotech) at 42°C overnight and then washed sequentially in 2× SSC (1× SSC is 0.15 M NaCl plus 0.015 M sodium citrate), 0.1% SDS, 1× SSC, and 0.5× SSC. Hybridized arrays were scanned at maximal resolution on an Affymetrix 428 scanner at variable photomultiplier tube voltage settings. Fluorescence intensity values from Cy3 channels were processed using Imagene 4.2 software (Biodiscovery). Normalized values were obtained by MAVI software (version Pro 2.5.1; MWG Biotech).

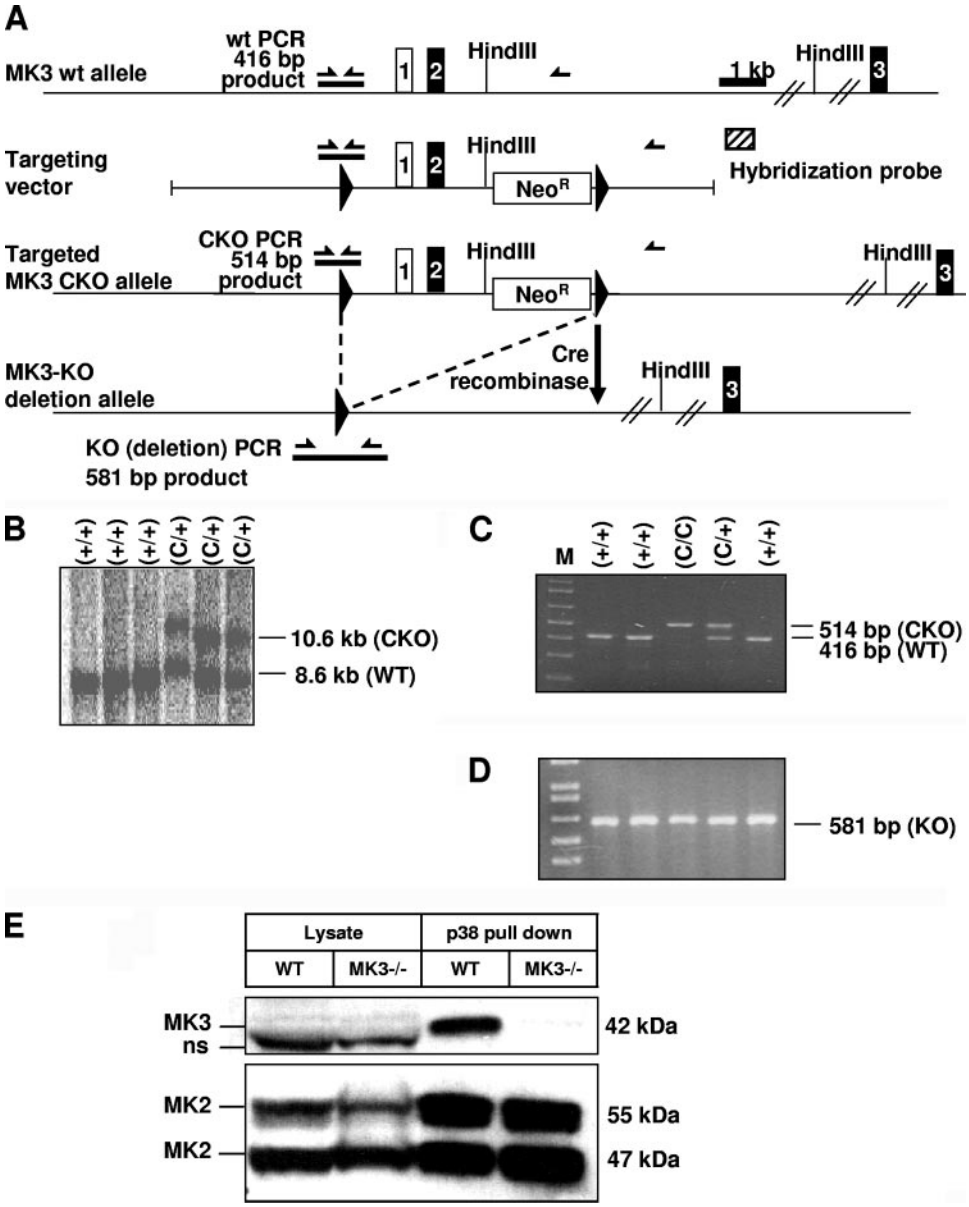

FIG. 1. Gene targeting strategy of MK3 deletion and absence of MK3 protein in MK3$^{-/-}$ tissues. (A) The MK3-CKO construct is composed of a 7-kb fragment of the MK3 gene with a 3-kb short arm and a 4-kb long arm flanking exons 1 and 2 and the neomycin resistance selectable marker gene (Neo^r). Exons 1 and 2 and Neo^r are flanked with LoxP sites as indicated by solid triangles. Positions of the Hind III restriction sites are indicated. Also indicated are positions of PCR primers, amplicons, and product sizes used for genotyping. (B) Southern blot analysis showing wild-type (+/+) and targeted (+/C) ES cell clones. PCR genotyping results from different sets of tail biopsies distinguishing WT (+) and conditional (C/C and C/+) alleles. (D) PCR results identifying KO (−) alleles after the MK3 KO allele was converted via germ line Cre-mediated deletion by crossing protamine-Cre transgenic mice (129SvEvBrd) with MK3-CKO mice. (E) Endogenous MK3 and MK2 were precipitated from 1 mg of spleen lysates by means of recombinant GST-p38 bound to glutathione-Sepharose 4B. Beads and 0.2 mg of whole lysates were subjected to SDS-PAGE and Western blotting using anti-MK3 antiserum (upper blot) and anti-MK2 antibodies (lower blot). There is a specific 42-kDa MK3 band precipitated from WT tissues which completely disappears in MK3$^{-/-}$ tissues. Endogenous MK3 is not detectable in whole cell lysates.ns, nonspecific band.

Heat map visualization was performed by importing log 2-transformed ratio data into the Mayday program (http://www.zbit.uni-tuebingen.de/pas/mayday/mayday.html).

Real-time PCR. cDNA prepared in parallel to the microarray experiments was used to validate selected results by real-time PCR. Assays on demand (Applied Biosystems; detailed information is in parentheses) for the following transcripts were used: β-actin (Actb; Mm00607939_s1), IκB-α (Nfkbia; Mm00477798_m1), Cxcl1 (Mm00433859_m1), c-Jun (Jun; Mm00495062_s1), and Csf2 (Mm00438328_m1). PCR was performed on an ABI7500 real-time PCR instrument. The threshold cycle (C_T) for each individual PCR product was calculated by the instrument software, and C_T values obtained for Nfkbia, Cxcl1, Jun, and Csf2 were normalized by subtracting the C_T values obtained for Actb to obtain ΔC_T values. Mean values were calculated from two to four C_T measurements; the standard error of the mean for all corresponding C_T values was less than 0.2. Relative expression of each mRNA was calculated by the $\Delta\Delta C_T$ method assuming a PCR efficiency of two.

LPS treatment of mice. LPS from *Escherichia coli* serotype 026:B6 (Sigma) was diluted in pyrogen-free saline, and 5 mg per kg of body weight was injected

intraperitoneally into five mice of each genotype. Ninety minutes after injection mice were sacrificed. Spleens were isolated and immediately frozen in liquid nitrogen. Spleen lysates were prepared using kinase assay lysis buffer and analyzed by Western blotting as described above. Serum cytokines were quantified by ELISA or by a Multi-Spot cytokine assay as described above.

RESULTS

Generation and characterization of MK3 knockout mice. The MK3 gene was targeted in mice by homologous recombination in ES cells, resulting in insertion of a floxed gene region spanning exons 1 and 2 and containing a neomycin cassette (Fig. 1A and B) and generation of MK3 CKO mice (Fig. 1C). The MK3 KO allele was converted via germ line Cre-mediated deletion by crossing protamine-Cre transgenic mice (129SvEvBrd) with MK3-CKO mice (Fig. 1D). MK3$^{-/-}$ KO mice are viable and fertile and do not display abnormalities in tissue morphology or behavior. To prove that deletion of the gene resulted in deletion of the encoded protein, we analyzed expression of MK3 in spleen cell lysates of WT and MK3$^{-/-}$ mice by Western blotting. No MK3 band could be detected in wild-type lysates, although MK2 detection was clearly possible (Fig. 1E, lysate). Since the sensitivities of the anti-MK3 and anti-MK2 antisera used are comparable (not shown), this indicates that in wild-type tissues expression of MK3 is much less than that of MK2. The MK3 mRNA expression level detected by reverse transcription-PCR is also much less than that of MK2 (data not shown). To overcome these technical problems and to specifically enrich p38-binding proteins, we used GST-p38 pull-down before MK3 Western blotting. For wild-type spleen cells (Fig. 1E) and other tissues (not shown), a specific band for MK3 can be detected in the pull-down, which is completely missing in MK3$^{-/-}$ cells. This indicates that the deleted gene results in complete loss of MK3 protein expression.

No significant changes in cytokine production, p38, and TTP levels in MK3$^{-/-}$ mice. The phenotype of MK2 deletion is very prominent, displaying defects in LPS-induced endotoxic reactions and cytokine production (16), reduction of p38 (17) and TTP levels (15), defects in chemotaxic cell migration (13), and increased susceptibility to infection (19). Since MK3 exhibits evolutionary, structural, and apparent extensive functional similarities to MK2 (12), we analyzed the phenotype of MK3 deficiency in regard to cytokine production, p38, and TTP level. In contrast to MK2 knockout mice and cells, MK3$^{-/-}$ mice did not show a decrease either in LPS-induced production of the cytokines IL-12p40, IL-6, KC (IL-8), IL-10, IL-1, RANTES, GM-CSF, gamma interferon, monocyte chemoattractant protein 1, and TNF or in IL-6 mRNA stability (not shown). Furthermore, in MK3-deficient macrophages (Fig. 2) and in different MK3$^{-/-}$ tissues (not shown), the protein levels of p38 and TTP were not significantly changed compared to the WT, and expression and activation of MK2 were not significantly altered (Fig. 2). Hence, MK3 deletion resulted in a phenotype clearly different from the complex inflammation-impaired phenotype of mice deficient in MK2 in spite of the extensive structural and regulatory similarities of MK2 and MK3. This discrepancy could be explained by different spatial-temporal expression of both enzymes.

MK3 and MK2 are ubiquitously expressed and phosphorylated in parallel upon LPS stimulation. We analyzed protein

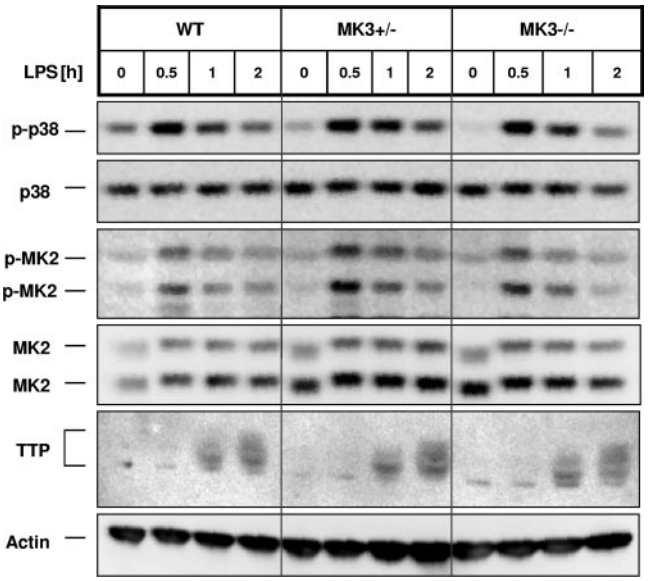

FIG. 2. Analysis of p38/MK2 signaling in MK3-deficient macrophages. There were no significant changes in p38 MAPK, MK2, and TTP expression and phosphorylation levels in MK3-deficient cells. Peritoneal macrophages from WT, MK3$^{+/-}$, and MK3$^{-/-}$ mice were serum starved for several hours and then stimulated with 10 ng/ml LPS for the times indicated. Lysates were then immunoblotted for total and phosphorylated p38 MAPK and MK2 and with an antiserum that recognizes both the phosphorylated and nonphosphorylated forms of TTP.

expression of MK3 and MK2 in different mouse tissues from wild-type and MK2-deficient mice by using GST-p38 pull-down to enrich endogenous MK3 and MK2 and to avoid nonspecific bands in subsequent Western blot detection. MK3 protein migrating with an apparent molecular mass of 42 kDa is ubiquitously expressed at different levels in the tissues analyzed (Fig. 3A, upper blot). High levels of MK3 could be detected in the spleen, lung, and skeletal muscle. The pattern of MK3 expression is similar to MK2, which is detected on the same blot as additional bands with apparent molecular masses of 47 and 55 kDa (Fig. 3A, lower blot). There is no difference in MK3 expression between MK2$^{-/-}$ and WT tissues.

Next we analyzed the phosphorylation of MK3 at one of its regulatory phosphorylation sites located in the activation loop of the kinase, threonine T203 in mouse, using an antiserum against phospho-T222 of human MK2 (Fig. 3 B). This antiserum is well suited to detect both mouse phospho-T208-MK2 and phospho-T203-MK3. A 42-kDa band specific for MK3 is phosphorylated in response to LPS, is reduced in macrophages from MK3$^{+/-}$ animals, and disappears in MK3$^{-/-}$ macrophages (Fig. 3C). It can be seen that MK3 phosphorylation upon LPS stimulation of primary macrophages has dynamics similar to p38 activation (Fig. 2) and MK2 phosphorylation, with the maximum reached after about 30 min and a subsequent decrease.

Detection of stress-stimulated catalytic activity of MK3 in MK2-deficient cells. To find out whether MK3 is activated in response to stress stimuli other than LPS, we stimulated primary WT and MK2-deficient MEFs with arsenite. Phosphorylation of MK2 as well as MK3 upon arsenite treatment can be demonstrated by Western blotting using the anti-phospho-

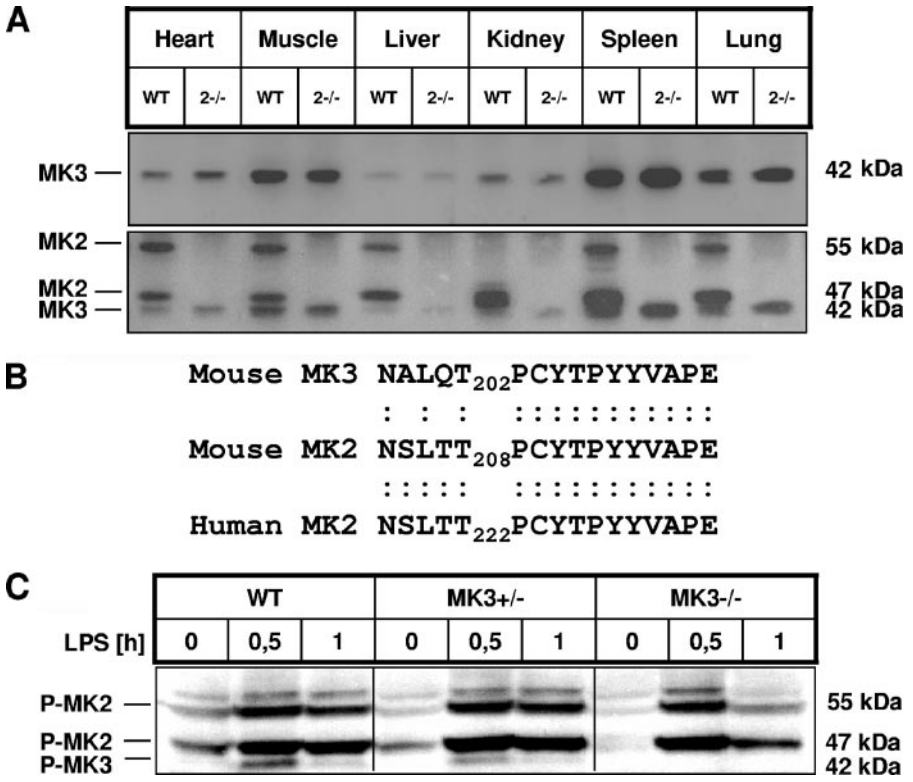

FIG. 3. Analysis of MK2 and MK3 expression and phosphorylation. MK3 expression in different tissues. GST-p38 was bound to glutathione-Sepharose 4B (Amersham Pharmacia Biotech). The beads were incubated with the lysates from different WT and MK2$^{-/-}$ tissues. (A) The blot was developed against MK3 using anti-MK3-specific antiserum. The same blot was redeveloped against MK2 using anti-MK2 antibodies. (B) Comparison of the phosphorylation sites of MK2 and MK3, recognized by the phospho-specific antiserum against human phospho-T222 MK2 (MK2 pT222). (C) Detection of phospho-MK2 and phospho-MK3 in LPS-stimulated macrophages by Western blotting. Peritoneal macrophages from WT, MK3$^{+/-}$, and MK3$^{-/-}$ mice were serum starved for several hours and then stimulated with 10 ng/ml LPS for the times indicated. Lysates were then immunoblotted using antibodies against phosphorylated MK2 (pT222) that recognize the phosphorylated MK3 as well (see panel B).

T222-MK2 antibodies. In WT cells both phospho-MK2 (55 and 47 kDa) and phospho-MK3 (42 kDa) are detected, while in MK2-deficient MEFs only arsenite-stimulated phosphorylation of MK3 can be seen (Fig. 4A). Endogenous MK2 and MK3 were precipitated from WT and MK2$^{-/-}$ cells by GST pull-down using a catalytically dead mutant of p38, GST-p38-AFG, and were assayed in an in vitro kinase reaction with recombinant small heat shock protein Hsp25 as a substrate. As a negative control, pull-down was carried out with GST alone. In WT cells, where both MK2 and MK3 are precipitated, a strong induction of kinase activity upon arsenite stimulation can be seen (Fig. 4B). In MK2$^{-/-}$ cells, Hsp25 phosphorylation is significantly reduced but still detectable and stimulated by the p38 activator arsenite (Fig. 4B). Quantification of Hsp25 phosphorylation by phosphorimaging revealed about 10 to 20% activity for MK3 in the MK2-deficient cells, corresponding approximately to the ratio of MK2/MK3 phospho-protein levels. To prove that this remaining kinase activity in MK2-deficient cells is due to MK3, we performed an in-gel kinase assay with Hsp25 as the substrate polymerized into the gel to visualize the electrophoretic mobility of the kinase activities precipitated by catalytically dead GST-p38-AGF. Three bands representing arsenite-stimulated Hsp25 kinase activity can be detected: two bands correspond to the 47-kDa and 55-kDa isoforms of MK2 and disappear in MK2$^{-/-}$ cells; the third weak 42-kDa band corresponds to MK3 and is also detectable in MK2-deficient MEFs (Fig. 4C). These findings support the notion that MK2 and MK3 are both activated upon stress and display catalytic activity against Hsp25.

Overexpression of MK3 compensates for MK2 deficiency. According to the observations above, we made the hypothesis that MK2 and MK3 display the same mechanism of activation and substrate specificity in vivo and that the differences between the phenotypes of MK3- and MK2-deficient mice result from differences in the levels of expression of MK3 and MK2. To prove this idea, we tested whether MK3 overexpression can rescue the phenotype of MK2-deficient cells. To do so, we established a retrovirus-based transduction system for fibroblasts providing transduction efficiency of up to 98%. cDNAs coding for MK3, MK2, and an MK2 catalytically dead mutant, MK2-K76R, were cloned into the retroviral expression vector pMMP-IRES-EGFP, which contains an IRES between the gene of interest and a region coding for enhanced GFP (EGFP). The polycistronic mRNA encoded by this vector leads to the translation of the protein of interest and EGFP independently and enables us to determine the degree of transduction by fluorescence measurement using fluorescence-activated cell sorting. In this experiment, we stimulated WT and MK2$^{-/-}$ cells transduced with MK3, MK2, MK2-K76R, or empty vector with arsenite. The cells were lysed, and expres-

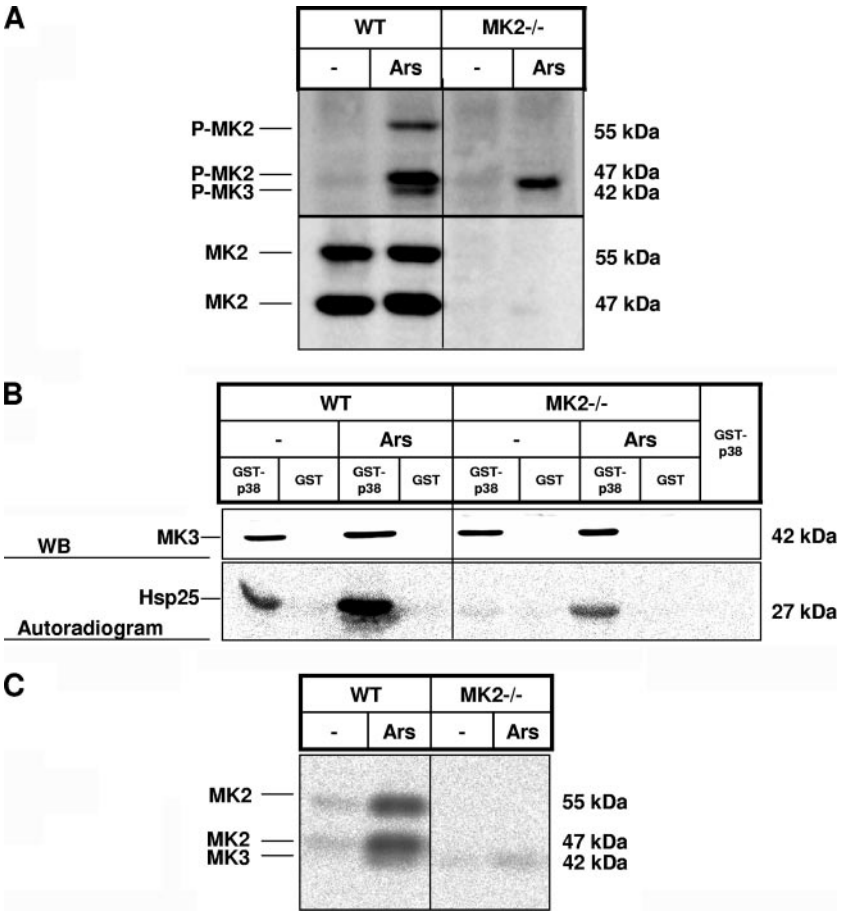

FIG. 4. In vivo phosphorylation and activation of MK3 by arsenite. Primary WT and MK2$^{-/-}$ MEF cells were starved overnight and then stimulated with 200 μM arsenite (Ars) for 30 min. The protein lysates were prepared. (A) The lysates were immunoblotted for phosphorylated MK2/MK3 and for total MK2. (B) MK2/MK3 kinase activity against recombinant Hsp25. Endogenous MK2 and MK3 were precipitated indirectly by using catalytically dead mutant GST-p38 (TGY/AGF) coupled to glutathione-Sepharose beads. The beads were used in a kinase reaction with recombinant Hsp25 as a substrate. The reaction mixture was resolved by SDS-PAGE immunoblotted for MK3 (WB), and then Hsp25 phosphorylating activity was detected by phosphorimaging (autoradiogram). (C) In-gel Hsp25 kinase assay of precipitates from GST-p38 (TGY/AGF) pull-down in WT and MK2$^{-/-}$ MEFs.

sion of MK2, GFP, Hsp25, p38, and GAPDH and the phosphorylation of MK2/3 and Hsp25 were analyzed by Western blotting (Fig. 5A). Almost all MK2-deficient MEFs were transduced (not shown) and expressed EGFP to comparable degrees (Fig. 5A, anti-GFP). Both MK3 and MK2 are expressed in the transduced cells to comparable degrees and their phosphorylated forms can be detected to comparable levels (Fig. 5A, anti-phospho-MK2). Notably, ectopic expression of full-length MK2 cDNA results in only one of the two bands characteristic of endogenous MK2. Both transduced MK3 and MK2 show arsenite-dependent stimulation of phosphorylation at the activation loop, indicating the same mechanism of stress-dependent activation of both enzymes. To compare the in vivo substrate specificity of MK3 and MK2, we examined the phosphorylation of endogenous Hsp25 by an antibody detecting phospho-S86. Overexpression of both MK3 and MK2, but not catalytically dead MK2 or EGFP, rescues phosphorylation of endogenous Hsp25 at this site to a significant degree (Fig. 5A, band P-Hsp25). In addition, MK3, similar to MK2, shows interaction with and chaperoning properties for p38α MAPK, increasing its intracellular level (Fig. 5A, p38 alpha). In a parallel experiment, cell lysates of the transduced MEFs were used for in vitro kinase assays using recombinant Hsp25 as a substrate (Fig. 5B). MK3 and MK2 phosphorylated recombinant Hsp25 with the same intensity as endogenous MK2. These data indicate functional congruence of MK2 and MK3 at least in regard to phosphorylation of endogenous Hsp25.

MK2 regulates gene expression of ARE-containing mRNAs at the posttranscriptional level by increasing both mRNA stability and translation (25, 39). To analyze whether functional redundancy between MK3 and MK2 also exists in their ability to stabilize specific mRNAs, we measured the influence of MK3 and MK2 on stability of mRNAs by a gene array approach. MK2-deficient MEFs were transduced by MK3 or MK2 as described above, and a selected set of inflammatory transcripts was analyzed after 2 h of LPS stimulation before and after 2 h of additional actinomycin-D (ActD) treatment to monitor transcript stability. As indicated by the heat map shown in Fig. 6A, a large number of these genes were upregulated by LPS treatment in the absence or presence of MK2 or

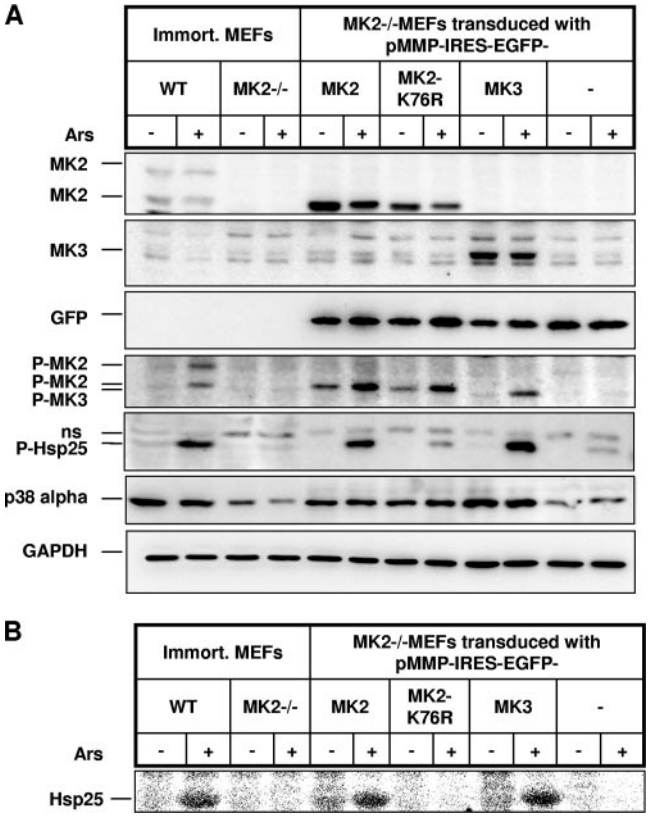

FIG. 5. Rescue of Hsp25 phosphorylation and p38 level in MK2-deficient MEFs by overexpression of MK3. MK2$^{-/-}$ immortalized MEF cells were transduced with pMMP-IRES-EGFP vector expressing EGFP in parallel with wild-type MK2, a catalytically dead mutant of MK2-K76R, or MK3 and as a negative control with empty vector expressing EGFP alone. Cells were starved overnight and then were left unstimulated (Ars−) or were stimulated for 40 min with 200 μM arsenite (Ars+). (A) In vivo rescue of Hsp25 phosphorylation and p38-alpha protein levels by overexpressed MK3. The lysates were immunoblotted for phosphorylated and total Hsp25 and p38-alpha and for phosphorylated MK2/3. As an expression control the lysates were immunoblotted for MK2, MK3, and GFP. (B) Cell lysates were incubated in vitro with recombinant Hsp25 and [γ-^{33}P]ATP, and Hsp25 phosphorylating activity was detected by phosphorimaging.

MK3. Twenty-eight genes were identified whose mRNA levels after ActD treatment ranged from 50% down to only 4% of the LPS-induced mRNA amounts in the absence of transcriptional inhibition, indicating various degrees of posttranscriptional mRNA stabilization. It is known that ARE-containing mRNAs are destabilized in the absence of MK2 activity (39). Accordingly, as shown in Fig. 6, the mRNA levels of several of these genes were increased after MK2 or MK3 was reintroduced. These effects were most prominent for cxcl1 (GROα) and csf2 (GM-CSF) whose mRNA levels in the presence of ActD increased by more than fivefold in MK2- or MK3-rescued cells. Of note, we also identified other unstable transcripts, such as c-jun or Nfkbia (IκB-α) that were either not stabilized or only very weakly stabilized by MK3 or MK2 (Fig. 6B). From this experiment it would seem that the ability of MK2 or MK3 to stabilize a subgroup of LPS-induced genes is largely redundant. This observation is confirmed by real-time PCR (Fig. 6B) and analysis of protein levels of CXCL1 (Fig. 6C). We mea-

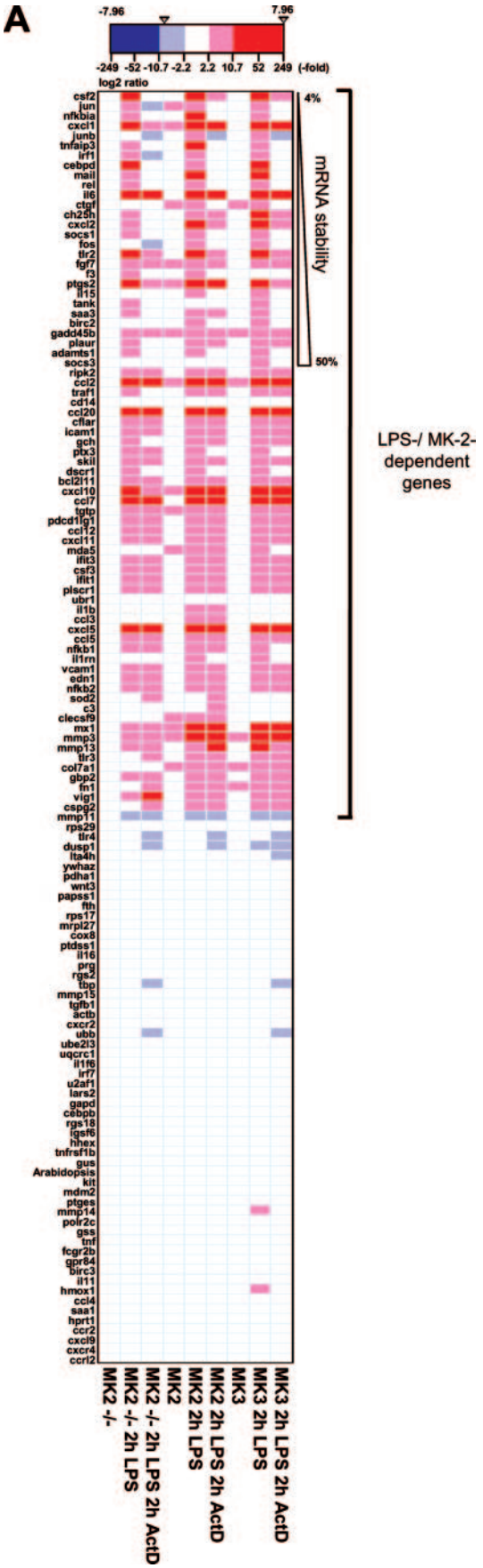

B

micro-array	ratios of gene gene expression relative to MK2 -/- cells									rescue by MK2	rescue by MK3	relative mRNA stability
gene	MK2 -/-	MK2 -/- 2h LPS	MK2 -/- 2h LPS 2h ActD	MK2	MK2 2h LPS	MK2 2h LPS 2h ActD	MK3	MK3 2h LPS	MK3 2h LPS 2h ActD	MK2 LPS ActD / MK2 -/- LPS ActD	MK3 LPS ActD / MK2 -/- LPS ActD	MK2 -/- LPS / MK2 -/- LPS ActD
csf2	1,0	29,0	1,1	1,3	95,0	9,2	1,0	80,0	5,8	8,2	5,2	25,8
jun	1,0	5,5	0,3	3,2	6,5	0,6	1,6	6,1	0,5	1,7	1,5	17,0
nfkbia	1,0	8,3	0,5	1,9	12,9	0,7	1,3	10,1	0,6	1,4	1,1	16,8
cxcl1	1,0	109,2	7,6	3,0	202,3	125,2	1,7	248,6	71,5	16,5	9,4	14,4

real-time PCR	ratios of gene gene expression relative to MK2 -/- cells									rescue by MK2	rescue by MK3	relative mRNA stability
gene	MK2 -/-	MK2 -/- 2h LPS	MK2 -/- 2h LPS 2h ActD	MK2	MK2 2h LPS	MK2 2h LPS 2h ActD	MK3	MK3 2h LPS	MK3 2h LPS 2h ActD	MK2 LPS ActD / MK2 -/- LPS ActD	MK3 LPS ActD / MK2 -/- LPS ActD	MK2 -/- LPS / MK2 -/- LPS ActD
csf2	1,0	1545,1	14,6	12,1	5004,5	356,6	2,1	4610,5	391,7	24,5	26,9	106,1
jun	1,0	3,9	0,1	2,8	7,8	0,4	2,9	3,7	0,5	2,8	3,8	26,8
nfkbia	1,0	6,9	0,2	1,4	10,7	0,1	1,3	8,1	0,3	0,8	1,9	43,5
cxcl1	1,0	294,0	11,4	4,2	794,6	185,5	2,0	992,6	213,8	16,3	18,8	25,9

induced by LPS | instable mRNAs | rescued by MK2 or by MK3

C

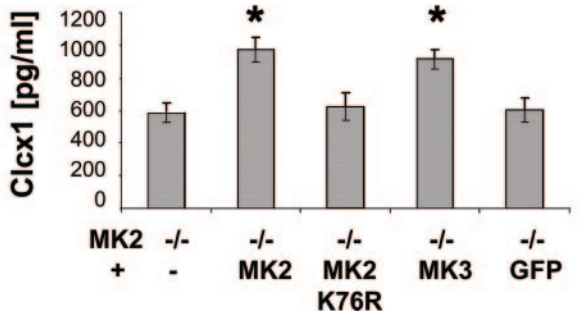

FIG. 6. Rescue of mRNA stability and stimulation of CXCL1 production in MK2-deficient MEFs by MK2 and MK3. (A) DNA microarray analysis of mRNA stability. cRNAs derived from the indicated samples were labeled with Cy3 and hybridized to 12 microarrays containing probes for 155 inflammatory genes including 19 housekeeping genes. A total of 129 genes with fluorescence intensity values of >100 in MK2-reconstituted cells stimulated with LPS were regarded as significantly expressed and selected for further analysis. Expression values of each indicated sample were divided by those of the MK2 KO control samples. The resulting ratios were log 2 transformed and are grouped according to dependence on MK2 and LPS (ratio of MK2 treated for 2 h with LPS/MK2$^{-/-}$ of >2.0) followed by their sensitivity to ActD treatment in the absence of MK2 as an indirect indicator of mRNA stability (ratio of MK2 $^{-/-}$ treated for 2 h with LPS/MK2 $^{-/-}$ treated for 2 h with LPS and for 2 h with ActD). Transcripts whose mRNA levels decreased by 50% (socs3) down to 4% (csf2) are indicated. (B) Shown are the relative mRNA expression values for the four most unstable mRNAs as determined by microarray experiments or by real-time PCR (C) CXCL1 production of LPS-stimulated MK2-deficient MEFs transduced with constructs coding for catalytically active MK2 and MK3, for MK2-K76R, and as control for GFP alone or nontransduced (−). Asterisks indicate statistically significant difference (single-sided t test, $P < 0.05$).

sured CXCL1 in the cell culture supernatant of MK2-deficient MEFs transduced with constructs coding for MK2, MK3, catalytically dead MK2-K76R, and GFP by ELISA. In MK2-deficient macrophages, there is LPS-induced production of CXCL1 protein, which is not detectable by ELISA before LPS treatment. In parallel to the stabilization of CXCL1 mRNA seen in Fig. 6A and B, both MK2 and MK3 are also able to increase CXCL1 production by MEFs (Fig. 6C). In contrast, the catalytically dead mutant of MK2 and GFP expression alone do not increase CXCL1 production, indicating a specific stimulatory effect of MK2 and MK3 catalytic activities on LPS-induced CXCL1 production by either their mRNA-stabilizing properties (Fig. 6A) or by translational stimulation. The influence of MK3 or MK2 on translation of specific mRNAs, such as TNF mRNA (25), cannot be measured using this experimental approach.

Generation and analysis of the MK2/MK3 double knockout. To further understand the biological significance of MK3 as well as the redundancy and compensation between MK2 and MK3, we crossed MK2- and MK3-deficient mice to establish the MK2/3 double-KO (DKO) strain. Unexpectedly, MK2/3-deficient animals show no defect in embryonic development, are viable, fertile, and, as far as we can judge, behave normally, indicating that there is no significant compensation between MK2 and MK3 necessary for development. In an MK2$^{+/-}$ × MK3$^{+/-}$ crossing, 6 of 82 F_1 animals are DKO, indicating no

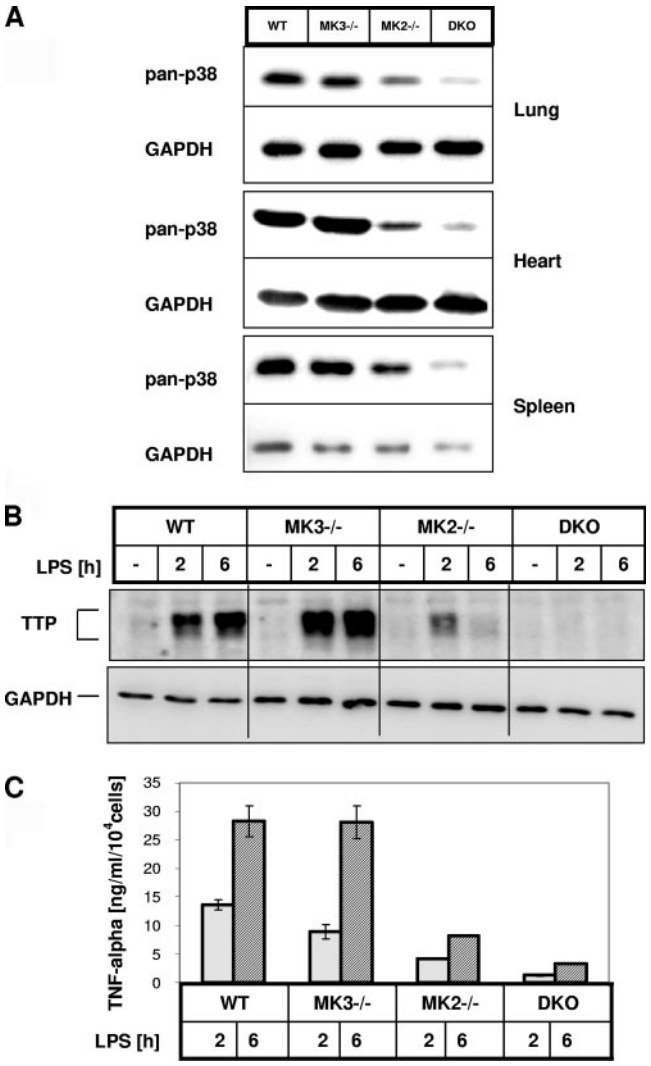

FIG. 7. Analysis of MK2/MK3 DKO mice. (A) Western blot detection of p38 MAPK levels in total lysates from MK2/MK3 DKO and, as controls, in MK2- and MK3-single knockout and WT mouse tissues. (B) Peritoneal-derived macrophages were stimulated with 1 μg/ml LPS for the times indicated. The TTP level in total lysates from WT, $MK2^{-/-}$, $MK3^{-/-}$, and MK2/MK3 DKO cells was analyzed by Western blotting. (C) TNF ELISA of macrophage culture supernatants. BMDMs were cultivated for 7 days, harvested, and counted, and equal numbers of cells were transferred to a 96-well plate. Cells were induced with 1 μg/ml LPS or left untreated as control for 2 and 6 h. TNF levels in the supernatants were measured by ELISA. For each genotype, three independent measurements were made; average and standard deviations are shown. The experiment is representative of two similar experiments.

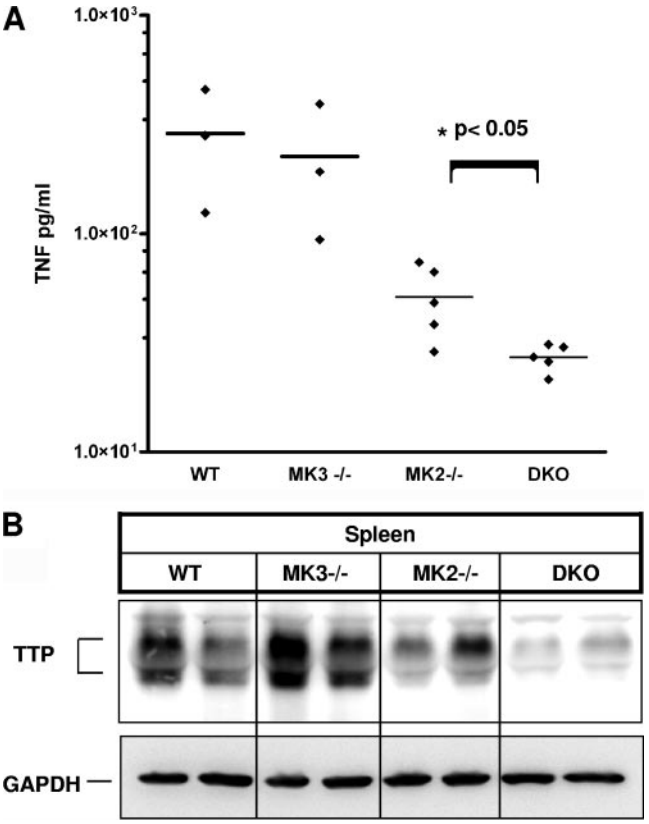

FIG. 8. Analysis of MK2/MK3 DKO mice in a septic shock in vivo model. Five animals of each genotype were injected intraperitoneally with LPS (5 mg per kg of body weight) diluted in PBS. Ninety minutes after injection mice were sacrificed, and serum and spleen were immediately isolated. (A) TNF level in serum was quantified by ELISA. A statistically significant difference between $MK2^{-/-}$ and DKO is indicated (single-sided *t* test, $P = 0.03$). (B) Spleen cell lysates were prepared using kinase assay lysis buffer and analyzed by Western blotting against TTP.

significant deviation from Mendelian ratio (1 out of 16 expected). Here we further analyzed MK2/3-deficient animals in regard to stabilization of p38 as well as TTP stabilization and TNF production in response to LPS.

It is already known that in several tissues, the absence of MK2 leads to a significant reduction of p38α protein level due to the missing MK2/p38α stabilizing complex formation (4, 17, 21, 34). In lung and heart tissue as well as in spleen cells, p38 protein levels are further reduced in the absence of both MK2 and MK3 (Fig. 7A). This indicates that MK3 is also able to form a stabilizing complex with p38, at least in the absence of MK2.

Another protein which is strongly affected in the MK2 knockout is TTP (15). We analyzed LPS-induced expression of TTP in peritoneal-derived macrophages by Western blotting. While in the MK3 knockout, no reduction of TTP expression after 2 and 6 h of LPS treatment can be detected, a clear difference is visible between MK2-deficient and DKO cells (Fig. 7B). This indicates that phosphorylation by MK3 contributes to TTP stabilization after LPS treatment.

The most prominent phenotype of MK2-deficient animals is their increased survival of endotoxic shock due to impaired TNF production (16). We analyzed TNF production of BMDM cultures derived from mice of the different genotypes. As expected, TNF production of MK2-deficient BMDMs is reduced about fivefold (Fig. 7C). In contrast, MK3-deficient macrophages show only a slight and not statistically significant reduction in TNF production. Interestingly, TNF production of DKO macrophages is further and significantly reduced compared to MK2-deficient cells, supporting the notion that MK3 can contribute to regulation of TNF biosynthesis.

Finally, we analyzed in vivo TNF production and TTP pro-

tein expression in LPS-challenged mice. Five animals of each genotype were injected with LPS, and after 90 min the TNF level in serum was determined by ELISA, and TTP level in spleen of two randomly chosen animals of each genotype was analyzed by Western blotting (Fig. 8 A and B). TNF production is significantly further impaired in DKO animals compared to MK2-deficient mice (single-sided t test, $P = 0.03$). Furthermore, semiquantitative detection of TTP protein in the spleen by Western blotting also supports the notion that TTP levels are further reduced in DKO compared to MK2-KO mice. These findings are consistent with the results obtained for macrophages in vitro.

DISCUSSION

Here, we analyzed the functional overlap between the two structurally related protein kinases MK2 and MK3 by a gene targeting approach. We provide evidence that both proteins tightly bind to p38, are coexpressed in the cells and tissues analyzed, are activated by the p38 pathway in response to stress (such as LPS or arsenite treatment) with comparable kinetics, and are able to phosphorylate endogenous small heat shock protein Hsp25. It is also demonstrated that in most cells and tissues analyzed (except skeletal muscle), MK3 expression is minor compared to MK2. Furthermore, MK3 enzymatic activity, probably as a result of the relatively low expression of the enzyme, is also minor compared to MK2 in the same cells. This becomes obvious when the activity of both enzymes is monitored by the same antibody against both activated forms of MK2 and MK3 after LPS treatment of peritoneal macrophages and also when the enzymatic activities of WT and MK2-deficient MEFs are compared after arsenite stimulation using an in-gel kinase assay. Hence, it is not surprising that the effects of the deletion of MK3 in the presence of MK2 are minor and difficult to detect.

Therefore, we decided to analyze the role of MK3 in an MK2-deficient background by analyzing how ectopic expression of MK2 and MK3 can rescue MK2 deficiency and by comparing the effects of the MK2 knockout and MK2/MK3 double knockout. We demonstrate that both MK2 and MK3 expression can rescue Hsp25 phosphorylation depending on the catalytic activity of the enzyme, while MK2 and MK3 stabilize p38 to a similar degree as the catalytically inactive mutant of MK2, confirming the idea that binding between both proteins leads to stabilization (17, 34). Furthermore, stabilization of the same group of LPS-responsive fibroblast transcripts is obtained with ectopic MK2 and MK3, while other transcript stabilities are not changed by both enzymes. It is still open whether the transcript-stabilizing properties of both enzymes in this experimental system result from their catalytic activity or from their stabilization of p38. However, CXCL1 production of these cells can only be significantly increased by catalytically active MK2 and MK3. ARE-containing transcript stability has been previously assessed in a human system by microarray analysis (11). The study identified several p38 MAPK-stabilized ARE-containing transcripts by means of the p38 inhibitor SB203580. In the experiment shown in Fig. 6, p38 MAP-stabilized mRNAs can be rescued by MK2 or MK3 (e.g., cxcl1 and Groα) or remain unstable after ActD treatment independent of MK2/MK3 (e.g., JUN B). Although both studies use different experimental designs and cell systems, i.e., pharmacological inhibition of p38 MAPK in a monocytic cell line (THP-1) versus reconstituted MK2-deficient embryonic fibroblasts as shown here, these results suggest that MK2 or MK3 targets a subset of ARE-containing inflammatory mRNAs that are stabilized by the p38 MAPK pathway.

Comparing the MK2 knockout with the MK2/3 double knockout, we could show that MK3 stabilizes the remaining p38 level in the MK2-deficient background and that the role of MK3 in TTP and TNF regulation is qualitatively indistinguishable from the role of MK2. Taking into account that MK2 is an established therapeutic target of inflammatory diseases, such as rheumatoid arthritis (14), and that small-molecule MK2 inhibitors are under investigation, the finding that MK3 is indistinguishable from MK2 in its inflammatory function would favor MK2/3 dual inhibitors.

The fact that MK2/3-deficient DKO mice are viable and show no obvious defects in embryonic development was unexpected. We anticipated that MK2 and MK3 mutually compensate each other in development, since both enzymes were described to functionally interact with components of the developmentally relevant polycomb complex involved in chromatin remodeling (26, 37, 40); thus, we expected significant defects in the absence of both enzymes. Possibly a more detailed analysis of, e.g., stem cell development in these animals may be necessary to identify minor but physiologically relevant effects. The further reduction of p38 expression in MK2/3 DKO compared to MK2-deficient tissue is also remarkable. However, the remaining level of p38 is obviously sufficient to compensate the effects of embryonic lethality and placental development described for the p38 knockout mice (1, 2, 35). This is similar to the finding that hypomorphic alleles of another protein kinase, PDK1, which lead to expression of only 10% of the kinase, can rescue embryonic lethality of that enzyme (18) and is supported by the observation that arsenite-stimulated ATF1/CREB phosphorylation by the p38 downstream kinases MSK1/2 is not significantly reduced in MK2/3 DKO cells (N. Ronkina, A. Kotlyarov, and M. Gaestel, unpublished data).

From our comparison of MK2 and MK3 here as well as from comparison of their catalytic activities and substrate specificities (7), their regulation of subcellular localization (8, 26, 36), and their mode of activation by p38α/β (7), no significant difference in the functions of both enzymes can be detected so far. This is reminiscent of the situation of p38α and p38β, where p38α displays the major activity and p38β activity is minor and dispensable for signaling of the p38 pathway (3). In both cases, it is still enigmatic why both related enzymes have been stably maintained during evolution. MK2 and MK3 are both present in birds and mammals, while only one MK2/3 molecule is found in the lower vertebrates (12). It may well be that there is an exemption from coexpression of both enzymes in one tissue or cell type not tested so far, making only the expressed enzyme essential in these cells. Deletion of the enzyme from these potential cells in mice obviously does not lead to a noticeable phenotype; however, we cannot exclude the possibility that the effect of such specific MK3 function could be detected during a detailed and comprehensive analysis of the MK3-deficient animals. Another possibility could be the

activation of one of the two enzymes by an alternative mechanism, activator, and pathway, which is distinct from the p38 pathway and responds to other signals (e.g., of specific Toll-like receptors) and stimuli. However, this pathway and its physiological function are still to be identified.

ACKNOWLEDGMENTS

We thank Stefanie Schumacher, Jessica Schwermann, and Corinna Meier for plasmids pDEST15-alpha-p38, pMMP-IRES-GFP-MK2 and -MK2-K76R, and pGEX-5x-1-MK3, respectively; Jeffrey Pelker for the ELISA; and Heike Schneider for gene array support. Genotyping and mouse colony maintenance were done by Tatiana Iakovleva, Gretchen Ireland, Lauren Rusnak, and Brenda Lager.

This work was supported by Deutsche Forschungsgemeinschaft grant GA453/10-1 and by the European Community grant RTN-HPRN-CT-2002-00255.

REFERENCES

1. **Adams, R. H., A. Porras, G. Alonso, M. Jones, K. Vintersten, S. Panelli, A. Valladares, L. Perez, R. Klein, and A. R. Nebreda.** 2000. Essential role of p38α MAP kinase in placental but not embryonic cardiovascular development. Mol. Cell **6:**109–116.
2. **Allen, M., L. Svensson, M. Roach, J. Hambor, J. McNeish, and C. A. Gabel.** 2000. Deficiency of the stress kinase p38α results in embryonic lethality: characterization of the kinase dependence of stress responses of enzyme-deficient embryonic stem cells. J. Exp. Med. **191:**859–870.
3. **Beardmore, V. A., H. J. Hinton, C. Eftychi, M. Apostolaki, M. Armaka, J. Darragh, J. McIlrath, J. M. Carr, L. J. Armit, C. Clacher, L. Malone, G. Kollias, and J. S. Arthur.** 2005. Generation and characterization of p38β (MAPK11) gene-targeted mice. Mol. Cell. Biol. **25:**10454–10464.
4. **Ben-Levy, R., S. Hooper, R. Wilson, H. F. Paterson, and C. J. Marshall.** 1998. Nuclear export of the stress-activated protein kinase p38 mediated by its substrate MAPKAP kinase-2. Curr. Biol. **8:**1049–1057.
5. **Brook, M., C. R. Tchen, T. Santalucia, J. McIlrath, J. S. Arthur, J. Saklatvala, and A. R. Clark.** 2006. Posttranslational regulation of tristetraprolin subcellular localization and protein stability by p38 mitogen-activated protein kinase and extracellular signal-regulated kinase pathways. Mol. Cell. Biol. **26:**2408–2418.
6. **Chrestensen, C. A., M. J. Schroeder, J. Shabanowitz, D. F. Hunt, J. W. Pelo, M. T. Worthington, and T. W. Sturgill.** 2004. MAPKAP kinase 2 phosphorylates tristetraprolin on in vivo sites including Ser178, a site required for 14-3-3 binding. J. Biol. Chem. **279:**10176–10184.
7. **Clifton, A. D., P. R. Young, and P. Cohen.** 1996. A comparison of the substrate specificity of MAPKAP kinase-2 and MAPKAP kinase-3 and their activation by cytokines and cellular stress. FEBS Lett. **392:**209–214.
8. **Engel, K., A. Kotlyarov, and M. Gaestel.** 1998. Leptomycin B-sensitive nuclear export of MAPKAP kinase 2 is regulated by phosphorylation. EMBO J. **17:**3363–3371.
9. **Engel, K., H. Schultz, F. Martin, A. Kotlyarov, K. Plath, M. Hahn, U. Heinemann, and M. Gaestel.** 1995. Constitutive activation of mitogen-activated protein kinase-activated protein kinase 2 by mutation of phosphorylation sites and an A-helix motif. J. Biol. Chem. **270:**27213–27221.
10. **Freshney, N. W., L. Rawlinson, F. Guesdon, E. Jones, S. Cowley, J. Hsuan, and J. Saklatvala.** 1994. Interleukin-1 activates a novel protein kinase cascade that results in the phosphorylation of Hsp27. Cell **78:**1039–1049.
11. **Frevel, M. A., T. Bakheet, A. M. Silva, J. G. Hissong, K. S. Khabar, and B. R. Williams.** 2003. p38 mitogen-activated protein kinase-dependent and -independent signaling of mRNA stability of AU-rich element-containing transcripts. Mol. Cell. Biol. **23:**425–436.
12. **Gaestel, M.** 2006. MAPKAP kinases—MKs—two's company, three's a crowd. Nat. Rev. Mol. Cell. Biol. **7:**120–130.
13. **Hannigan, M. O., L. Zhan, Y. Ai, A. Kotlyarov, M. Gaestel, and C. K. Huang.** 2001. Abnormal migration phenotype of mitogen-activated protein kinase-activated protein kinase $2^{-/-}$ neutrophils in zigmond chambers containing formyl-methionyl-leucyl-phenylalanine gradients. J. Immunol. **167:**3953–3961.
14. **Hegen, M., M. Gaestel, C. L. Nickerson-Nutter, L.-L. Lin, and J.-B. Telliez.** 2006. MAPKAP kinase 2-deficient mice are resistant to collagen-induced arthritis. J. Immunol. **177:**1913–1917.
15. **Hitti, E., T. Iakovleva, M. Brook, S. Deppenmeier, A. D. Gruber, D. Radzioch, A. R. Clark, P. J. Blackshear, A. Kotlyarov, and M. Gaestel.** 2006. Mitogen-activated protein kinase-activated protein kinase 2 regulates tumor necrosis factor mRNA stability and translation mainly by altering tristetraprolin expression, stability, and binding to adenine/uridine-rich element. Mol. Cell. Biol. **26:**2399–2407.
16. **Kotlyarov, A., A. Neininger, C. Schubert, R. Eckert, C. Birchmeier, H. D. Volk, and M. Gaestel.** 1999. MAPKAP kinase 2 is essential for LPS-induced TNF-alpha biosynthesis. Nat. Cell Biol. **1:**94–97.
17. **Kotlyarov, A., Y. Yannoni, S. Fritz, K. Laass, J. B. Telliez, D. Pitman, L. L. Lin, and M. Gaestel.** 2002. Distinct cellular functions of MK2. Mol. Cell. Biol. **22:**4827–4835.
18. **Lawlor, M. A., A. Mora, P. R. Ashby, M. R. Williams, V. Murray-Tait, L. Malone, A. R. Prescott, J. M. Lucocq, and D. R. Alessi.** 2002. Essential role of PDK1 in regulating cell size and development in mice. EMBO J. **21:**3728–3738.
19. **Lehner, M. D., F. Schwoebel, A. Kotlyarov, M. Leist, M. Gaestel, and T. Hartung.** 2002. Mitogen-activated protein kinase-activated protein kinase 2-deficient mice show increased susceptibility to *Listeria monocytogenes* infection. J. Immunol. **168:**4667–4673.
20. **Ludwig, S., K. Engel, A. Hoffmeyer, G. Sithanandam, B. Neufeld, D. Palm, M. Gaestel, and U. R. Rapp.** 1996. 3pK, a novel mitogen-activated protein (MAP) kinase-activated protein kinase, is targeted by three MAP kinase pathways. Mol. Cell. Biol. **16:**6687–6697.
21. **Lukas, S. M., R. R. Kroe, J. Wildeson, G. W. Peet, L. Frego, W. Davidson, R. H. Ingraham, C. A. Pargellis, M. E. Labadia, and B. G. Werneburg.** 2004. Catalysis and function of the p38 alpha. MK2a signaling complex. Biochemistry **43:**9950–9960.
22. **Mahtani, K. R., M. Brook, J. L. Dean, G. Sully, J. Saklatvala, and A. R. Clark.** 2001. Mitogen-activated protein kinase p38 controls the expression and posttranslational modification of tristetraprolin, a regulator of tumor necrosis factor alpha mRNA stability. Mol. Cell. Biol. **21:**6461–6469.
23. **Manke, I. A., A. Nguyen, D. Lim, M. Q. Stewart, A. E. Elia, and M. B. Yaffe.** 2005. MAPKAP kinase-2 is a cell cycle checkpoint kinase that regulates the G2/M transition and S phase progression in response to UV irradiation. Mol. Cell **17:**37–48.
24. **McLaughlin, M. M., S. Kumar, P. C. McDonnell, S. Van Horn, J. C. Lee, G. P. Livi, and P. R. Young.** 1996. Identification of mitogen-activated protein (MAP) kinase-activated protein kinase-3, a novel substrate of CSBP p38 MAP kinase. J. Biol. Chem. **271:**8488–8492.
25. **Neininger, A., D. Kontoyiannis, A. Kotlyarov, R. Winzen, R. Eckert, H. D. Volk, H. Holtmann, G. Kollias, and M. Gaestel.** 2002. MK2 targets AU-rich elements and regulates biosynthesis of tumor necrosis factor and interleukin-6 independently at different post-transcriptional levels. J. Biol. Chem. **277:**3065–3068.
26. **Neufeld, B., A. Grosse-Wilde, A. Hoffmeyer, B. W. Jordan, P. Chen, D. Dinev, S. Ludwig, and U. R. Rapp.** 2000. Serine/threonine kinases 3pK and MAPK-activated protein kinase 2 interact with the basic helix-loop-helix transcription factor E47 and repress its transcriptional activity. J. Biol. Chem. **275:**20239–20242.
27. **Rouse, J., P. Cohen, S. Trigon, M. Morange, A. Alonso-Llamazares, D. Zamanillo, T. Hunt, and A. R. Nebreda.** 1994. A novel kinase cascade triggered by stress and heat shock that stimulates MAPKAP kinase-2 and phosphorylation of the small heat shock proteins. Cell **78:**1027–1037.
28. **Roux, P. P., and J. Blenis.** 2004. ERK and p38 MAPK-activated protein kinases: a family of protein kinases with diverse biological functions. Microbiol. Mol. Biol. Rev. **68:**320–344.
29. **Schumacher, S., K. Laass, S. Kant, Y. Shi, A. Visel, A. D. Gruber, A. Kotlyarov, and M. Gaestel.** 11 November 2004, posting date. Scaffolding by ERK3 regulates MK5 in development. EMBO J. **23:**4770–4779.
30. **Seternes, O. M., T. Mikalsen, B. Johansen, E. Michaelsen, C. G. Armstrong, N. A. Morrice, B. Turgeon, S. Meloche, U. Moens, and S. M. Keyse.** 2 December 2004, posting date. Activation of MK5/PRAK by the atypical MAP kinase ERK3 defines a novel signal transduction pathway. EMBO J. **23:**4780–4791.
31. **Sithanandam, G., F. Latif, F. M. Duh, R. Bernal, U. Smola, H. Li, I. Kuzmin, V. Wixler, L. Geil, and S. Shrestha.** 1996. 3pK, a new mitogen-activated protein kinase-activated protein kinase located in the small cell lung cancer tumor suppressor gene region. Mol. Cell. Biol. **16:**868–876.
32. **Stoecklin, G., T. Stubbs, N. Kedersha, S. Wax, W. F. Rigby, T. K. Blackwell, and P. Anderson.** 11 March 2004, posting date. MK2-induced tristetraprolin: 14-3-3 complexes prevent stress granule association and ARE-mRNA decay. EMBO J. **23:**1313–1324.
33. **Stokoe, D., D. G. Campbell, S. Nakielny, H. Hidaka, S. J. Leevers, C. Marshall, and P. Cohen.** 1992. MAPKAP kinase-2: a novel protein kinase activated by mitogen-activated protein kinase. EMBO J. **11:**3985–3994.
34. **Sudo, T., K. Kawai, H. Matsuzaki, and H. Osada.** 20 September 2005, posting date. p38 mitogen-activated protein kinase plays a key role in regulating MAPKAPK2 expression. Biochem. Biophys. Res. Commun. **337:**415–421.
35. **Tamura, K., T. Sudo, U. Senftleben, A. M. Dadak, R. Johnson, and M. Karin.** 2000. Requirement for p38alpha in erythropoietin expression: a role for stress kinases in erythropoiesis. Cell **102:**221–231.
36. **Tanoue, T., R. Maeda, M. Adachi, and E. Nishida.** 2001. Identification of a docking groove on ERK and p38 MAP kinases that regulates the specificity of docking interactions. EMBO J. **20:**466–479.
37. **Voncken, J. W., H. Niessen, B. Neufeld, U. Rennefahrt, V. Dahlmans, N. Kubben, B. Holzer, S. Ludwig, and U. R. Rapp.** 24 November 2004, posting date. MAPKAP kinase 3pK phosphorylates and regulates chromatin association of the polycomb group protein Bmi1. J. Biol. Chem. **280:**5178–5187.
38. **Wang, X., M. A. Khaleque, M. J. Zhao, R. Zhong, M. Gaestel, and S. K.**

Calderwood. 8 November 2005, posting date. Phosphorylation of HSF1 by MAPK-activated protein kinase 2 on serine 121, inhibits transcriptional activity and promotes HSP90 binding. J. Biol. Chem. **281:**782–791.

39. **Winzen, R., M. Kracht, B. Ritter, A. Wilhelm, C. Y. Chen, A. B. Shyu, M. Muller, M. Gaestel, K. Resch, and H. Holtmann.** 1999. The p38 MAP kinase pathway signals for cytokine-induced mRNA stabilization via MAP kinase-activated protein kinase 2 and an AU-rich region-targeted mechanism. EMBO J. **18:**4969–4980.
40. **Yannoni, Y. M., M. Gaestel, and L. L. Lin.** 2004. P66(ShcA) interacts with MAPKAP kinase 2 and regulates its activity. FEBS Lett. **564:**205–211.
41. **Zakowski, V., G. Keramas, K. Kilian, U. R. Rapp, and S. Ludwig.** 2004. Mitogen-activated 3p kinase is active in the nucleus. Exp. Cell Res. **299:**101–109.